Experimental Animals
Exp. Anim. 71(4), 433–441, 2022

Original

A novel ENU-induced *Cpox* mutation causes microcytic hypochromic anemia in mice

Yuki MIYASAKA[1)], Kento OKUDA[1)], Ikuo MIURA[2)], Hiromi MOTEGI[3)], Shigeharu WAKANA[2, 4)] and Tamio OHNO[1)]

[1)]*Division of Experimental Animals, Graduate School of Medicine, Nagoya University, 65 Tsurumai-cho, Showa-ku, Nagoya, Aichi 466-8550, Japan*
[2)]*Technology and Developmental Team for Mouse Phenotype Analysis, RIKEN BioResource Research Center, 3-1-1 Koyadai, Tsukuba, Ibaraki 305-0074, Japan*
[3)]*Team for Advanced Development and Evaluation of Human Disease Models, RIKEN BioResource Research Center, 3-1-1 Koyadai, Tsukuba, Ibaraki 305-0074, Japan*
[4)]*Department of Animal Experimentation, Foundation for Biomedical Research and Innovation at Kobe, Creative Lab for Innovation in Kobe, 5F 6-3-7, Minatojima-Minamimachi, Chuo-ku, Kobe, Hyogo 650-0047, Japan*

Abstract: Mouse models of red blood cell abnormalities are important for understanding the underlying molecular mechanisms of human erythrocytic diseases. DBA.B6-*Mha* (Microcytic hypochromic anemia) congenic mice were generated from the cross between *N*-ethyl-*N*-nitrosourea (ENU)-mutagenized male C57BL/6J and female DBA/2J mice as part of the RIKEN large-scale ENU mutagenesis project. The mice were established by backcrossing with DBA/2J mice for more than 20 generations. These mice showed autosomal-dominant microcytic hypochromic anemia with decreased mean corpuscular volume (MCV) and mean corpuscular hemoglobin (MCH) levels and increased red blood cell distribution width (RDW) and plasma ferritin levels. Linkage analysis indicated that the *Mha* locus was located within an interval of approximately 1.95-Mb between *D16Nut1* (58.35 Mb) and *D16Mit185* (60.30 Mb) on mouse chromosome 16. Mutation analysis revealed that DBA.B6-*Mha* mice had a point mutation (c.921-2A>G) at the acceptor site of intron 4 in the coproporphyrinogen oxidase (*Cpox*) gene, a heme-synthesizing gene. RT-PCR revealed that the *Cpox* mRNA in DBA.B6-*Mha* mice caused splicing errors. Our results suggest that microcytic hypochromic anemia in DBA.B6-*Mha* mice is owing to impaired heme synthesis caused by splice mutations in *Cpox*. Therefore, the DBA.B6-*Mha* mice may be used to elucidate the molecular mechanisms underlying microcytic hypochromic anemia caused by mutations in *Cpox*. Although low MCV levels are known to confer malarial resistance to the host, there were no marked changes in the susceptibility of DBA.B6-*Mha* mice to rodent malarial (*Plasmodium yoelii* 17XL) infection.
Key words: coproporphyrinogen oxidase (*Cpox*) gene, malaria, mice, microcytic hypochromic anemia, *N*-ethyl-*N*-nitrosourea (ENU) mutagenesis

Introduction

N-ethyl-*N*-nitrosourea (ENU) is a potent alkylating mutagen that introduces a high rate of random genome-wide point mutations into the mouse germline by affecting the premeiotic spermatogonial germ cells in the testes [1]. ENU-induced point mutations cause a wide variety of aberrations, including complete or partial loss of gene function [1]. Since human and mouse genomes are highly homologous, and approximately 70% of the disease-causing alleles in humans arise due to point mutations [2], large-scale ENU mutagenesis screens in mice have been employed to study human diseases [3]. The combination of such screens and a forward genetics ap-

(Received 10 March 2022 / Accepted 12 April 2022 / Published online in J-STAGE 9 May 2022)
Corresponding author: T. Ohno. email: ohno@med.nagoya-u.ac.jp
Supplementary Tables: refer to J-STAGE: https://www.jstage.jst.go.jp/browse/expanim

proach can lead to the identification of novel genes, pathways, and their functions in disease pathogenesis [1].

ENU mutagenesis screening has also contributed to the establishment of mouse models of red blood cell abnormalities for the analysis of gene function in red blood cells. For example, ankryin-1 (*Ank1*) (RBC2 [4] and ENU7192 [5]), β-globin (RBC13 [6] and RBC14 [6]), and triosephosphate isomerase 1 (RBC19 [7]) mutants were identified by ENU mutagenesis screening in mice to identify new mouse models and novel genes or alleles in red blood cells. These mice are used as animal models for hereditary spherocytosis, β-thalassemia, and hematological defects associated with triosephosphate isomerase deficiency. The analyses of these mice have provided novel insights into their function in red blood cells. In addition, mouse models of hereditary red blood cell abnormalities help researchers understand the relationship between malarial parasites, which infect red blood cells, and host erythrocytic genes. Several ENU-induced mutant mice with mutations in erythrocytes, such as *Ank1* [4], adenosine monophosphate deaminase 3 [8], and hydroxymethylbilane synthase [9], have been used in research pertaining to malaria.

M100835 mice were generated from the cross between ENU-mutagenized male C57BL/6J and female DBA/2J mice as part of the RIKEN large-scale ENU mutagenesis project. These mice showed autosomal-dominant red blood cell abnormalities (microcytic hypochromic anemia) with decreased mean corpuscular volume (MCV) and mean corpuscular hemoglobin (MCH) levels, and increased red blood cell distribution width (RDW) levels. The *Mha* (Microcytic hypochromic anemia) locus was identified to be located between rs3089786 (38.93 Mb) and rs4197051 (66.15 Mb) on mouse chromosome 16 using genome-wide single-nucleotide polymorphism (SNP) mapping of second-backcross generation (N_2) M100835 mice obtained by crossing first-generation (G_1) males with female DBA/2J mice by the RIKEN BioResource Research Center (RIKEN BRC, Tsukuba, Japan).

In this study, we investigated the hematological phenotypes of DBA.B6-*Mha* congenic mice, which were established by backcrossing male M100835 mice with female DBA/2J mice for more than 20 generations and identified the causative gene that causes microcytic hypochromic anemia in the *Mha* locus by fine-mapping and mutation analysis of chromosome 16. In addition, we analyzed the susceptibility of DBA.B6-*Mha* mice to malaria.

Materials and Methods

Experimental animals and ethical approval

DBA/2J mice (*Mus musculus*) were purchased from CLEA Japan (Tokyo, Japan). C57BL/6J mice were purchased from Japan SLC (Hamamatsu, Japan). M100835 mice were generated by crossing ENU-mutagenized male C57BL/6J and female DBA/2J mice for dominant mutant screening using the Riken Genomic Sciences Research Complex (RIKEN GSC, Yokohama, Japan). M100835 (N_3) mice (BRC no. RBRC-GSC0129) backcrossed with DBA/2J mice were obtained from RIKEN BRC (http://www.brc.riken.jp/lab/animal/en/gscmouse.shtml). DBA.B6-*Mha* congenic mice (formal name: DBA.B6-*D16Nut5-D16Mit139*) were established by backcrossing male M100835 mice with female DBA/2J mice for more than 20 generations at the Institute for Laboratory Animal Research, Graduate School of Medicine, Nagoya University, Japan. Heterozygous M100835 mice were crossed with one another to obtain 34 offspring; none of these were homozygous for the *Mha* allele, and it was assumed that the allele was lethal. Heterozygous and wild-type (DBA/2J) mice obtained by backcrossing were used in all experiments.

All the mice were fed a commercial CE-2 diet (CLEA Japan) and had *ad libitum* access to water. Mice were bred in a pathogen-free facility at the Institute for Laboratory Animal Research, Graduate School of Medicine, Nagoya University, and were maintained at a controlled temperature of 23 ± 1°C, humidity of 55 ± 10%, and a light cycle of 12 h light (from 09:00 to 21:00)/12 h dark (from 21:00 to 09:00). All animal care and experimental procedures were approved by the Animal Care and Use Committee of the Graduate School of Medicine, Nagoya University, and were conducted in accordance with Nagoya University Regulations on Animal Care and Use in Research.

Analysis of hematological phenotypes

Blood was collected from the hearts of deeply anesthetized male and female DBA/2J and DBA.B6-*Mha* (N_{23}) mice at 8 weeks of age and stored in tubes containing heparin (heparin sodium injection: 5,000 units/5 ml; MOCHIDA, Mochida Pharmaceutical Co., LTD., Tokyo, Japan). Hematological examinations were performed using an automatic blood analyzer (VetScan HM5; Abaxis, Europe, Darmstadt, Germany). Plasma ferritin was measured using the Mouse Ferritin ELISA Kit (ab157713; Abcam, Cambridge, UK) according to the manufacturer's protocol and read on a benchmark plate reader (Bio-Rad, Hercules, CA, USA).

 doi: 10.1538/expanim.22-0032

Genetic mapping

Genetic mapping of *Mha* locus was performed using the 30 mice with the highest and lowest MCV from N_3 to N_{20}, obtained by backcrossing M100835 with DBA/2J mice. Genomic DNA was extracted from mice pinnae using the KAPA Express Extract (Kapa Biosystems, Woburn, MA, USA) and genotyped using GoTaq Green Master mix (Promega, Madison, WI, USA), seven microsatellite markers, and four indel markers (Supplementary Table 1) on chromosome 16. The PCR amplification conditions were as follows: 35 cycles of 95°C for 30 s, 55°C for 30 s, and 72°C for 30 s. The products were subjected to 4% agarose gel (NuSieve, 3:1 Agarose; Lonza, Tokyo, Japan) electrophoresis and stained with ethidium bromide (Nippon Gene, Tokyo, Japan).

Mutation analysis

Mutation analysis was performed on the genomic DNA from DBA/2J, C57BL/6J, and DBA.B6-*Mha* mice. The PCR products of coproporphyrinogen oxidase (*Cpox*) gene in these mice were amplified using GoTaq Green Master mix (Promega) and primer sets (Supplementary Table 1) to amplify the coding regions and exon/intron junctions in *Cpox*. The PCR products were purified using ExoSAP-IT (Thermo Fisher Scientific, Waltham, MA, USA). A mutation in DBA.B6-*Mha* mice was detected by performing Sanger DNA sequencing of the purified PCR products using the BigDye Terminator v3.1 Cycle Sequencing Kit (Thermo Fisher Scientific) and a 3730xl DNA Analyzer (Thermo Fisher Scientific) by Eurofins Genomics K.K (Tokyo, Japan).

Detection of *Cpox* mutant alleles in DBA.B6-*Mha* mice

A novel *Cpox* mutation in DBA.B6-*Mha* mice was detected using PCR-restriction fragment length polymorphism (PCR-RFLP) analysis. The mutation site (the acceptor site of intron 4) in *Cpox* was amplified using the primer sets, *Cpox*_Int4F2 and *Cpox*_Ex5R (Supplementary Table 1). The amplification conditions were as follows: 35 cycles at 95°C for 30 s, 65°C for 30 s, and 72°C for 30 s. The products were digested with *Xsp*I (Takara Bio, Kusatsu, Japan) at 37°C for 1 h. They were then subjected to 2% agarose gel (Lonza) electrophoresis and stained with ethidium bromide (Nippon Gene). Mice used for the hematological (n=51) and rodent malaria susceptibility analyses (n=36) were confirmed the genotype of *Cpox* using this method.

RT-PCR, quantitative RT-PCR (qRT-PCR) and cDNA sequencing

Total RNA was isolated from the bone marrow cells of DBA.B6-*Mha*, DBA/2J, and C57BL/6J mice, at 8 weeks of age, using the PureLink RNA Mini Kit (Life Technologies, Grand Island, NY, USA), according to the manufacturer's protocol. Total RNA was treated with DNase I (Nippon Gene) and cDNA was generated using a Superscript VILO cDNA Synthesis Kit (Life Technologies). RT-PCR was performed using KOD Fx neo (TOYOBO, Osaka, Japan), *Cpox*-specific primer sets (*Cpox*_Ex3F and *Cpox*_Ex7R), and hypoxanthine-guanine phosphoribosyltransferase (*Hprt*)-specific primer sets (*Hprt*_Ex4F and *Hprt*_Ex5R) (Supplementary Table 1). The amplification conditions were as follows: 94°C for 2 min, followed by 35 cycles at 98°C for 10 s and 68°C for 30 s. The products were then subjected to 2% agarose gel (Lonza) electrophoresis and stained with ethidium bromide (Nippon Gene).

qRT-PCR was performed using a QuantiFast SYBR Green PCR Kit (Qiagen, Valencia, CA, USA), *Cpox*-specific primer sets (*Cpox*_Ex1F2 and *Cpox*_Ex2R), and *Hprt*-specific primer sets (*Hprt*_Ex4F and *Hprt*_Ex5R) (Supplementary Table 1) according to the manufacturer's protocol. The products were analyzed using a LightCycler 480 Instrument II (Roche Diagnostics, Tokyo, Japan). Signals specific to *Cpox* were normalized to those specific to *Hprt*. The expression levels of the genes in C57BL/6J mice were assigned an arbitrary value of one, for comparison.

cDNA sequencing was performed using cDNA generated from bone marrow cells of DBA.B6-*Mha* mice at 8 weeks of age. RT-PCR products of *Cpox* gene in DBA.B6-*Mha* mice were amplified using Platinum *Taq* DNA Polymerase High Fidelity (Thermo Fisher Scientific) and primer sets, *Cpox*_Ex6F and *Cpox*_Ex7R2 (Supplementary Table 1), which amplified the SNP (rs4190612) in the 3′-untranslated region (UTR). Purification and sequencing of RT-PCR products were performed as described above.

Rodent malaria infections

Rodent malarial parasite infections were performed as described previously [10, 11]. Red blood cells infected with the rodent malarial parasite, *Plasmodium yoelii* 17XL (*P. yoelii* 17XL), were stored as frozen stocks at −80°C. Freshly thawed parasitized red blood cells were passaged once using DBA/2J mice. Male and female DBA/2J and DBA.B6-*Mha* mice at 8 weeks of age were infected by an intraperitoneal injection of 1×10^5 parasitized red blood cells from the passaged mice. The percentage of parasitized red blood cells was determined at 3 (72 h) and 5 (120 h) days post infection using thin blood smears stained with Giemsa (Merck Millipore, Darmstadt, Germany). Thin blood smears were observed

under a light microscope (BX53; Olympus, Tokyo, Japan), and the percentage of parasitized red blood cells was determined by dividing the number of infected red blood cells by the total number of red blood cells and multiplying by 100. The survival of the mice was monitored daily until 2 weeks post infection.

Statistical analyses

The link between genotype and phenotype was evaluated using the χ^2 test of independence. Hematological parameters, spleen and body weight, gene expression levels, and parasitemia levels are presented as mean ± SD. The two groups were compared using the Student's *t*-test. Survival rates were analyzed using the log-rank test. qRT-PCR data were analyzed using one-way analysis of variance with Tukey's post-hoc multiple comparison test. GraphPad Prism 6 (GraphPad, San Diego, CA, USA) was used to calculate the column statistics and compute *P* values; **P*<0.05, ***P*<0.01, ****P*<0.001 vs. DBA/2J mice; $^{\#\#\#}P$<0.001 vs. C57BL/6J mice.

Results

Hematological phenotypes in DBA.B6-*Mha* mice

We tested the hematological parameters of DBA.B6-*Mha* congenic mice established by backcrossing male M100835 mice with female DBA/2J mice for 23 generations. MCV and MCH levels were significantly lower, and the RDW-coefficient of variation (CV) and plasma ferritin levels were significantly higher in DBA.B6-*Mha* mice than in DBA/2J mice (Tables 1 and 2). These results suggest that the red blood cell abnormality observed in DBA.B6-*Mha* mice was microcytic hypochromic anemia caused by defective globin genes (hemoglobinopathies or thalassemia), defective heme synthesis, or decreased iron availability. The body and spleen weights of the DBA.B6-*Mha* and DBA/2J mice were not significantly different (Supplementary Table 2).

Genetic mapping of the *Mha* locus

The *Mha* locus was found to be located between the rs3089786 (38.93 Mb) and rs4197051 (66.15 Mb) regions on mouse chromosome 16. We performed fine mapping within this region using mice from generations N_3 to N_{20}. MCV levels were more clearly separated between the DBA/2J and M100835 mice. Therefore, we used MCV levels as a phenotypic indicator for fine mapping. This analysis revealed that the genotypes, *D16Nut5* (58.44 Mb), *D16Nut3* (58.57 Mb), and *D16Nut2* (59.31 Mb) correlated completely with MCV levels (Fig. 1A). Therefore, the causative mutation in the *Mha* locus was found to be located within an interval of approximately 1.95-Mb between *D16Nut1* (58.35 Mb) and *D16Mit185* (60.30 Mb) on C57BL/6J-derived chromosome 16 (Fig. 1A).

Table 1. Comparison of hematological parameters (mean ± SD) between DBA/2J and DBA.B6-*Mha* mice

Parameters	Female			Male		
	DBA/2J (n = 12)	DBA.B6-*Mha* (n = 12)	Change ratio[a)] (%)	DBA/2J (n = 18)	DBA.B6-*Mha* (n = 9)	Change ratio (%)
WBC (×10^9/l)	5.19 ± 2.56	5.19 ± 2.67	1.8	5.74 ± 3.53	4.54 ± 2.41	20.4
RBC (×10^{12}/l)	8.88 ± 0.96	9.92 ± 0.99*	11.7	9.28 ± 0.91	9.76 ± 1.26	5.2
HGB (g/dl)	12.35 ± 1.29	11.83 ± 1.33	4.3	13.15 ± 1.40	11.38 ± 1.19**	13.5
HCT (%)	41.69 ± 5.34	40.13 ± 4.50	3.7	44.47 ± 5.38	39.37 ± 4.94*	11.5
MCV (fl)	46.83 ± 1.59	40.58 ± 1.56***	13.4	47.89 ± 2.14	40.56 ± 3.61***	15.3
MCH (pg)	13.91 ± 0.43	11.93 ± 0.39***	14.3	14.18 ± 0.56	11.70 ± 0.41***	17.5
MCHC (g/dl)	29.74 ± 1.72	29.52 ± 1.52	0.8	29.72 ± 1.87	28.96 ± 1.73	2.6
RDW-SD (fl)	35.68 ± 1.15	36.13 ± 1.74	1.3	36.38 ± 1.96	36.30 ± 3.86	0.2
RDW-CV (%)	19.13 ± 0.32	22.70 ± 0.42***	18.7	19.05 ± 0.41	22.63 ± 0.46***	18.0
PLT (×10^4/μl)	296.67 ± 87.86	363.00 ± 139.46	23.2	310.50 ± 77.16	322.56 ± 135.53	3.9

**P*<0.05, ***P*<0.01 and ****P*<0.001 vs. DBA/2J (Student's *t*-test). [a)]Change ratio of parameters in DBA.B6-*Mha* mice with respect to that of DBA/2J mice.

Table 2. Comparison of plasma ferritin levels (mean ± SD) between DBA/2J and DBA.B6-*Mha* mice

Parameters	Female			Male		
	DBA/2J (n=12)	DBA.B6-*Mha* (n=9)	Change ratio[a)] (%)	DBA/2J (n=12)	DBA.B6-*Mha* (n=7)	Change ratio (%)
Plasma ferritin (ng/ml)	426.20 ± 76.56	634.67 ± 165.06**	48.9	364.29 ± 104.27	532.10 ± 139.66**	46.1

***P*<0.01 vs. DBA/2J (Student's *t*-test). [a)]Change ratio of parameters in DBA.B6-*Mha* mice with respect to that of DBA/2J mice.

 doi: 10.1538/expanim.22-0032

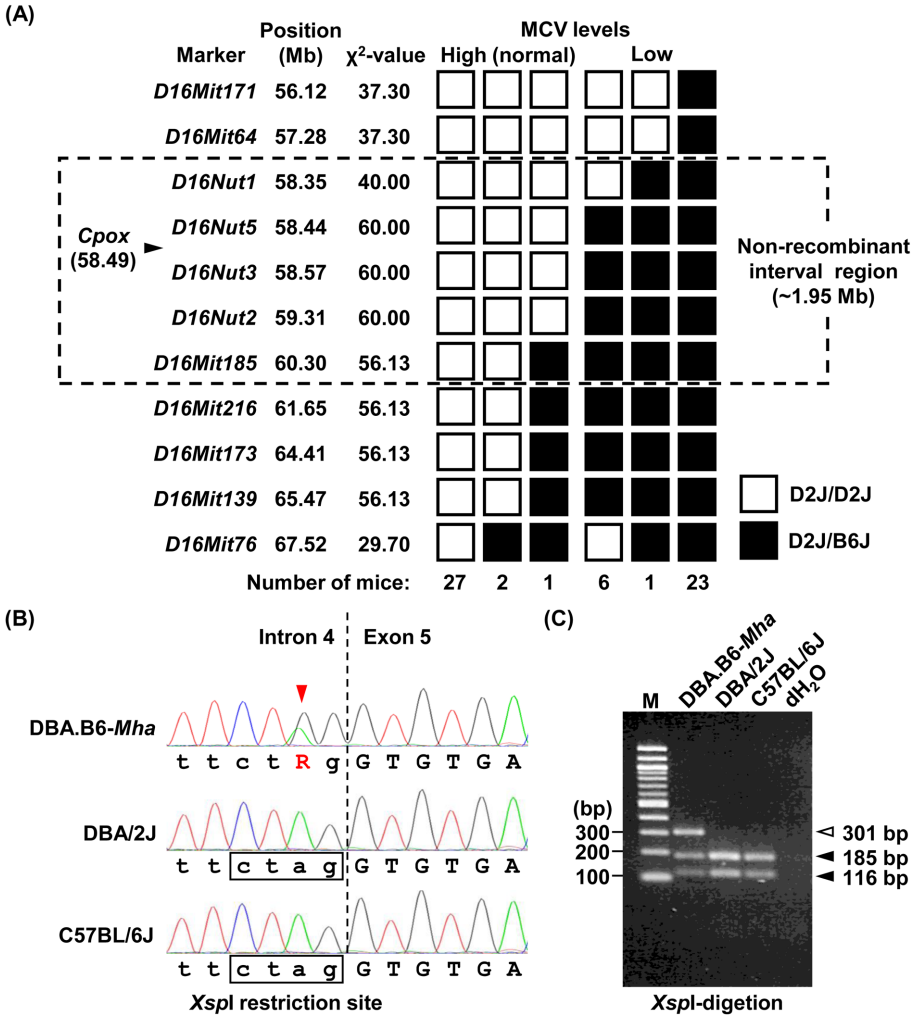

Fig. 1. Positional cloning in DBA.B6-*Mha* mice. (A) Linkage analysis of genes from N_3 to N_{20}, obtained by backcrossing M100835 with DBA/2J mice, between the *D16Mit171* (56.12 Mb) and *D16Mit76* (67.52 Mb) region on mouse chromosome 16. Markers, marker positions, and χ^2 values are shown on the left. The number of offspring inheriting each type of chromosome is listed at the bottom of each column. Open boxes and black boxes represent the homozygous DBA/2J (D2J/D2J) and heterozygous DBA/2J and C57BL/6J (D2J/B6J) genotypes, respectively. The dotted area indicates the non-recombinant interval region. (B) Mutation analysis of *Cpox* in DBA.B6-*Mha* mice. Sequencing analysis of intron 4 to exon 5 of *Cpox* in DBA.B6-*Mha* (top), DBA/2J (middle), and C57BL/6J (bottom) mice. A point mutation (A to G) at the acceptor site of intron 4 in *Cpox* is found in DBA.B6-*Mha* mice (red arrowhead). (C) Detection of $Cpox^{Mha}$ mutation using PCR-restriction fragment length polymorphism. C57BL/6J-derived *Cpox* alleles in DBA.B6-*Mha* mice lack the *Xsp*I restriction endonuclease sites in intron 4 to exon 5. The amplicon from DBA.B6-*Mha* mice was not partially digested by *Xsp*I and yielded 301, 185, and 116 bp bands. In contrast, DBA/2J and C57BL/6J mice carry the *Xsp*I restriction site, and the products obtained from both mice did not show the 301 bp band. M, 100 bp DNA ladder.

Mutation analysis of *Cpox* in DBA.B6-*Mha* mice

Cpox, which is located between the non-recombinant interval region (Fig. 1A), codes for the sixth enzyme in the heme biosynthesis pathway and catalyzes oxidative decarboxylation of coproporphyrinogen to protoporphyrinogen. *Cpox* is reported to cause microcytic hypochromic anemia with elevated serum ferritin levels in mice [12]. By sequencing *Cpox*, we identified a point mutation (c.921-2A>G, $Cpox^{Mha}$ mutation) at the acceptor site of intron 4 in C57BL/6J derived-*Cpox* in DBA.B6-*Mha* mice (Fig. 1B). No mutations were detected in the coding region or other exon/intron junctions of *Cpox*. In addition, we performed PCR-RFLP analysis using the *Xsp*I restriction endonuclease to confirm the $Cpox^{Mha}$ mutation. Intron 4 of the C57BL/6J derived-*Cpox* gene in DBA.B6-*Mha* mice lacked the *Xsp*I restriction endonuclease site because of the ENU-induced mutation (Fig. 1B). The PCR products that amplified intron 4 in *Cpox*

were separated into 301, 185, and 116 bp bands by *Xsp*I treatment (Fig. 1C). On the other hand, the 301 bp band was not detected in the *Xsp*I-treated PCR products from C57BL/6J and DBA/2J mice (Fig. 1C).

Cpox mRNA expression levels in DBA.B6-*Mha* mice

A $Cpox^{Mha}$ mutation was detected in the GU-AG consensus sequence, which is used for intron recognition in most cases of pre-mRNA splicing in eukaryotes [13]. Mutations at splice junctions often cause exon skipping, short deletions, or insertions in mature mRNAs [14]. To investigate whether the $Cpox^{Mha}$ mutation leads to splicing errors, we performed RT-PCR using the primer sets, *Cpox*_Ex3F and *Cpox*_Ex7R, designed for exons 3 to 7, to amplify the exon 4 to 5 junction in *Cpox* (Fig. 2). A single band (560 bp) of *Cpox* mRNA was detected in C57BL/6J and DBA/2J mice, whereas multiple bands (560 bp, larger and smaller) were detected in DBA.B6-*Mha* mice (Fig. 2).

Next, we measured total *Cpox* mRNA levels in the bone marrow cells of DBA.B6-*Mha* mice. In qRT-PCR analysis with *Cpox*-specific primer sets designed for exons 1 and 2, the total *Cpox* mRNA levels in C57BL/6J mice were approximately four times higher than those in DBA/2J mice (Fig. 3A), whereas the total *Cpox* mRNA levels in DBA.B6-*Mha* mice were comparable to those in DBA/2J mice (Fig. 3A) despite carrying the C57BL/6J-derived *Cpox* allele. In addition, in the double peaks of SNP (rs4190612, guanine, or adenine), in the 3′-UTR obtained by cDNA sequencing analysis of *Cpox* in DBA.B6-*Mha* mice, C57BL/6J-derived guanine peaks were lower than DBA/2J-derived adenine peaks (Fig. 3B).

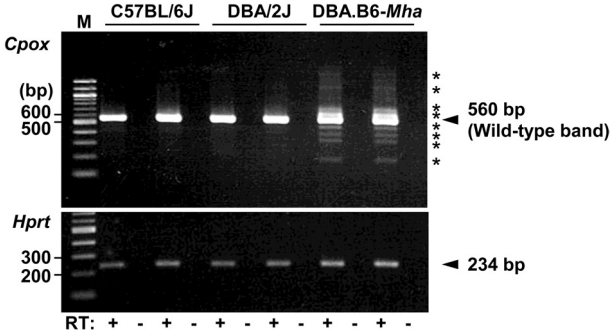

Fig. 2. *Cpox* mRNA transcription in DBA.B6-*Mha* mice. RT-PCR analysis of *Cpox* in the bone marrow cells of C57BL/6J, DBA/2J, and DBA.B6-*Mha* mice. Upper panel shows the RT-PCR products from *Cpox*-specific primers located in exons 3 and 7. A 560 bp band was detected in C57BL/6J and DBA/2J mice, whereas a 560 bp band, and multiple larger and smaller bands were detected in DBA.B6-*Mha* mice. Asterisks indicate aberrant transcripts. The integrity of the cDNA was confirmed using an *Hprt* control band (234 bp, bottom panel). M, 100 bp DNA ladder; RT, reverse transcription.

Susceptibility to rodent malarial parasite, *P. yoelii* 17XL infection in DBA.B6-*Mha* mice

To investigate the malaria susceptibility of DBA.B6-*Mha* (N_{23}) mice, we infected these mice with the lethal type of rodent malarial parasite, *P. yoelii* 17XL. Given the clear differences in malarial susceptibility in mice between the sexes [15], we compared parasitemia and survival rates of DBA/2J and DBA.B6-*Mha* mice within the same sex. No significant differences were de-

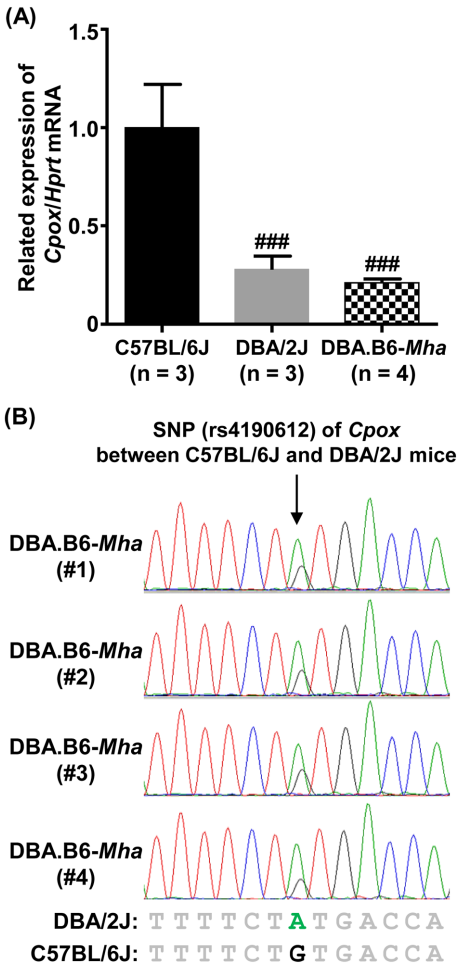

Fig. 3. Total *Cpox* expression levels in DBA.B6-*Mha* mice. (A) Relative expression levels of *Cpox* mRNA in the bone marrow cells in C57BL/6J (black box), DBA/2J (gray box), and DBA.B6-*Mha* (plaid box) mice. *Cpox* mRNA expression was measured by quantitative RT-PCR analysis using *Cpox*-specific primers located in exons 1 and 2. The expression levels in C57BL/6J mice were assigned an arbitrary value of 1 for comparative purposes. $^{###}P<0.001$ vs. C57BL/6J mice (one-way analysis of variance with Tukey's post-hoc multiple comparison test). (B) cDNA sequence waveform of *Cpox* 3′-untranslated region (UTR) in DBA.B6-*Mha* mice. An SNP (rs4190612, guanine or adenine) is found in the *Cpox* 3′-UTR region in C57BL/6J and DBA/2J mice. In double-peaks of this SNP obtained by cDNA sequencing analysis in four DBA.B6-*Mha* mice, the C57BL/6J-derived guanine peaks (black) were lower than the DBA/2J-derived adenine peaks (green) in each individual.

 doi: 10.1538/expanim.22-0032

tected in the levels of parasitemia in mice of both groups, 3 and 5 days post-infection (Figs. 4A and B). Only one female DBA.B6-*Mha* mouse survived for 2 weeks (Fig. 4C). However, there was no significant difference in the survival rates after *P. yoelii* 17XL infection between the DBA/2J and DBA.B6-*Mha* mice (Figs. 4C and D).

Discussion

DBA.B6-*Mha* mice exhibited autosomal-dominant microcytic hypochromic anemia with elevated plasma ferritin levels (Tables 1 and 2). Genetic mapping suggested that the *Mha* locus in DBA.B6-*Mha* mice is located within an interval of approximately 1.95-Mb between *D16Nut1* (58.35 Mb) and *D16Mit185* (60.30 Mb) on mouse chromosome 16 (Fig. 1A). DBA.B6-*Mha* mice had a point mutation (c.921-2A>G) at the acceptor site of intron 4 in *Cpox*, which is located between the non-recombinant interval region (Fig. 1B), and aberrant transcripts were detected in their *Cpox* mRNA (Fig. 2). *Cpox* is a heme-synthesizing gene and the causative gene for microcytic hypochromic anemia with elevated serum ferritin levels in mice [12]. Therefore, it was suggested that microcytic hypochromic anemia in DBA.B6-*Mha* mice was due to impaired heme synthesis caused by a splice mutation in *Cpox*. Based on these results, the congenic strain is renamed DBA.B6-$Cpox^{Mha}$.

In RT-PCR analysis of *Cpox*, 560 bp and multiple bands were detected in DBA.B6-$Cpox^{Mha}$ mice (Fig. 2). The total *Cpox* mRNA levels in DBA.B6-$Cpox^{Mha}$ mice were comparable to those in DBA/2J mice, despite carrying the C57BL/6J-derived and highly expressed *Cpox* allele (Fig. 3A). The double peaks of SNP (rs4190612, guanine, or adenine) in the 3′-UTR obtained by cDNA sequencing analysis of *Cpox* in DBA.B6-$Cpox^{Mha}$ mice showed that the C57BL/6J-derived guanine peaks were lower than the DBA/2J-derived adenine peaks (Fig. 3B). These results estimated that most of the 560 bp band detected in DBA.B6-$Cpox^{Mha}$ mice was a transcript produced from the DBA/2J (wild-type) alleles, and multiple aberrant transcripts produced from the C57BL/6J (ENU-induced mutant) alleles suffered from nonsense mutation-mediated mRNA decay.

Two mutant alleles of *Cpox* ($Cpox^{W373X}$ and $Cpox^{nct}$) have been reported in mice [12, 16]. $Cpox^{W373X}$ is a functional null allele that results in the loss of CPOX activ-

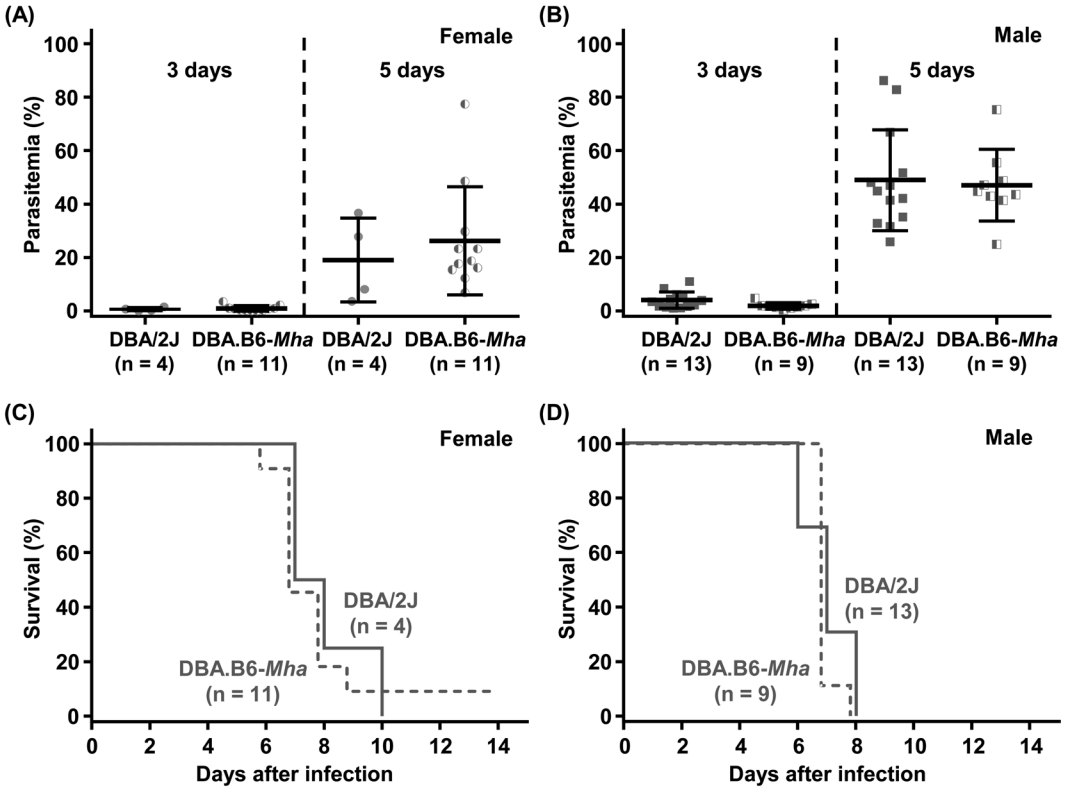

Fig. 4. Comparison of the susceptibility to rodent malarial parasite, *Plasmodium yoelii* 17XL infection of DBA/2J and DBA.B6-*Mha* mice. (A, B) Parasitemia 3 and 5 days post-infection with *P. yoelii* 17XL of (A) female DBA/2J (gray circles) and DBA.B6-*Mha* (half open gray circles), and (B) male DBA/2J (gray squares) and DBA.B6-*Mha* (half open gray squares) mice. Bold and thin lines represent the mean and SD, respectively. (C, D) Survival rates post-infection with *P. yoelii* 17XL of (C) female and (D) male DBA/2J (gray line) and DBA.B6-*Mha* (doted gray line) mice.

ity. Homozygous *Cpox*^{W373X} mice exhibit embryonic lethality at E9.5, whereas heterozygous mice develop microcytic hypochromic anemia with elevated serum ferritin levels [12]. *Cpox*^{nct} is a hypomorphic allele that reduces CPOX activity to approximately 15% of the normal level [16]. Although there is no information on hematological phenotypes, *Cpox*^{nct} homozygous mice are viable, unlike *Cpox*^{W373X} and DBA.B6-*Cpox*^{Mha} homozygous mice. *Cpox*^{nct} mice develop cataracts [16, 17], whereas DBA.B6-*Cpox*^{Mha} mice do not. The phenotypes of DBA.B6-*Cpox*^{Mha} mice were similar to those of *Cpox*^{W373X} mice, but not to those of *Cpox*^{nct} mice. Therefore, it was estimated that the *Cpox*^{Mha} mutation is a functional null mutation, and the microcytic hypochromic anemia of DBA.B6-*Cpox*^{Mha} mice is due to haploinsufficiency of CPOX.

Given the function of CPOX, microcytic hypochromic anemia in DBA.B6-*Cpox*^{Mha} mice is thought to be due to impaired heme synthesis. For example, patients with *ALAS2* mutation, which encodes an enzyme that catalyzes the first step in the heme biosynthetic pathway, develop microcytic hypochromic anemia (iron-loading anemia) caused by defective heme synthesis. Their anemia is characterized by a decrease in MCV and MCH, and an increase in RDW and serum ferritin levels [18, 19]. Schmitt *et al*. [20] reported that some mutations in the *CPOX* gene cause harderoporphyria and that patients show iron-loading anemia caused by the accumulation of harderoporphyrinogen, an intermediate porphyrin of the CPOX reaction and/or heme deficiency in red blood cell progenitors. According to American Board of Internal Medicine (ABIM) (https://www.abim.org/), outliers are diagnosed when MCV (median: 89.0 fl), MCH (median: 31.5 pg), RDW-CV (median: 11.8%) and ferritin (median: 165.5 ng/ml in female/180.0 ng/ml in male) levels change by approximately 10.1%, 11.1%, 23.4% and 86.1% in female/86.7% in male, respectively, from the median of the reference range in human. Female and male DBA.B6-*Cpox*^{Mha} mice showed a decrease in MCV of 13.4% and 15.3%, a decrease in MCH of 14.3% and 17.5%, an increase in RDW-CV of 18.7% and 18.0%, and an increase in plasma ferritin levels of 48.9% and 46.1%, respectively (Tables 1 and 2). Although the increase in RDW-CV and ferritin levels is not very significant compared to that of humans, changes in hematological parameters in DBA.B6-*Cpox*^{Mha} mice are similar to trends in iron-loading anemia caused by defective heme synthesis in humans. Thus, DBA.B6-*Cpox*^{Mha} mice may be used as a mouse model for iron-loaded anemia in harderoporphyria. Unfortunately, we were unable to investigate the accumulation of porphyrins and their precursors, including harderoporphyrinogen. Porphyrins are typically detected using high-performance liquid chromatography; however, we did not have this technology. There are no test kits available to detect these compounds in mice. In the future, it will be necessary to investigate the accumulation of harderoporphyrinogens in DBA.B6-*Cpox*^{Mha} mice.

Red blood cell abnormalities confer protective effects against malaria [21, 22]. A lower MCV is linked to reduced growth or invasion of malarial parasites [23, 24] and is attributed to the selection of malaria resistance [23, 25]. Goheen *et al*. [25] reported that parasite growth rates decrease by 1.4% for every 1 fl decrease in MCV levels in red blood cells from patients carrying the sickle-cell trait. *Ank1* and β-spectrin mutant mice show an approximate 15% and 10% reduction in MCV levels, respectively, and acquire resistance to malaria [26–28]. Although the MCV levels of DBA.B6-*Cpox*^{Mha} mice were 14.4% (for male and female combined) lower than those of DBA/2J mice (Table 1), there was no significant difference in the parasitemia or survival rates after *P. yoelii* 17XL infection between DBA/2J and DBA.B6-*Cpox*^{Mha} mice (Fig. 4). Hence, we conclude that a decreased MCV does not always confer malarial resistance.

In conclusion, the results of this study suggest that microcytic hypochromic anemia in DBA.B6-*Cpox*^{Mha} mice is caused by impaired heme synthesis due to a splice mutation in intron 4 of *Cpox*. Since DBA.B6-*Cpox*^{Mha} congenic mice were backcrossed with DBA/2J mice for more than 20 generations, a comparative analysis between DBA.B6-*Cpox*^{Mha} and DBA/2J mice will be useful in future studies as a tool for elucidating the molecular mechanisms of microcytic hypochromic anemia caused by mutations in *Cpox*.

Acknowledgments

We would like to thank the staff of the Division of Experimental Animals, Nagoya University Graduate School of Medicine for their technical support. We would also like to thank the staff of the Division for Medical Research Engineering, Nagoya University Graduate School of Medicine for their support with qRT-PCR.

References

1. Acevedo-Arozena A, Wells S, Potter P, Kelly M, Cox RD, Brown SD. ENU mutagenesis, a way forward to understand gene function. Annu Rev Genomics Hum Genet. 2008; 9: 49–69. [Medline] [CrossRef]
2. Cordes SP. *N*-ethyl-*N*-nitrosourea mutagenesis: boarding the mouse mutant express. Microbiol Mol Biol Rev. 2005; 69: 426–439. [Medline] [CrossRef]
3. Nolan PM, Hugill A, Cox RD. ENU mutagenesis in the mouse: application to human genetic disease. Brief Funct Genomics

Proteomics. 2002; 1: 278–289. [Medline] [CrossRef]
4. Rank G, Sutton R, Marshall V, Lundie RJ, Caddy J, Romeo T, et al. Novel roles for erythroid *Ankyrin-1* revealed through an ENU-induced null mouse mutant. Blood. 2009; 113: 3352–3362. [Medline] [CrossRef]
5. Hughes MR, Anderson N, Maltby S, Wong J, Berberovic Z, Birkenmeier CS, et al. A novel ENU-generated truncation mutation lacking the spectrin-binding and C-terminal regulatory domains of *Ank1* models severe hemolytic hereditary spherocytosis. Exp Hematol. 2011; 39: 305–320, 320.e1–320.e2. [Medline] [CrossRef]
6. Brown FC, Scott N, Rank G, Collinge JE, Vadolas J, Vickaryous N, et al. ENU mutagenesis identifies the first mouse mutants reproducing human β-thalassemia at the genomic level. Blood Cells Mol Dis. 2013; 50: 86–92. [Medline] [CrossRef]
7. Conway AJ, Brown FC, Hortle EJ, Burgio G, Foote SJ, Morton CJ, et al. Bone marrow transplantation corrects haemolytic anaemia in a novel ENU mutagenesis mouse model of *TPI* deficiency. Dis Model Mech. 2018; 11: dmm034678. [Medline] [CrossRef]
8. Hortle E, Nijagal B, Bauer DC, Jensen LM, Ahn SB, Cockburn IA, et al. Adenosine monophosphate deaminase 3 activation shortens erythrocyte half-life and provides malaria resistance in mice. Blood. 2016; 128: 1290–1301. [Medline] [CrossRef]
9. Schnider CB, Yang H, Starrs L, Ehmann A, Rahimi F, Di Pierro E, et al. Host porphobilinogen deaminase deficiency confers malaria resistance in *Plasmodium chabaudi* but not in *Plasmodium berghei* or *Plasmodium falciparum* during intraerythrocytic growth. Front Cell Infect Microbiol. 2020; 10: 464. [Medline] [CrossRef]
10. Ohno T, Miyasaka Y, Kuga M, Ushida K, Matsushima M, Kawabe T, et al. Mouse NC/Jic strain provides novel insights into host genetic factors for malaria research. Exp Anim. 2019; 68: 243–255. [Medline] [CrossRef]
11. Miyasaka Y, Niwa S, Masuya T, Ishii R, Kobayashi M, Horio F, et al. E3 ubiquitin ligase RNF123-deficient mice exhibit reduced parasitemia and mortality in rodent malaria (*Plasmodium yoelii* 17XL) infection. Parasitol Int. 2022; 88: 102542. [Medline] [CrossRef]
12. Conway AJ, Brown FC, Fullinfaw RO, Kile BT, Jane SM, Curtis DJ. A mouse model of hereditary coproporphyria identified in an ENU mutagenesis screen. Dis Model Mech. 2017; 10: 1005–1013. [Medline]
13. Breathnach R, Benoist C, O'Hare K, Gannon F, Chambon P. Ovalbumin gene: evidence for a leader sequence in mRNA and DNA sequences at the exon-intron boundaries. Proc Natl Acad Sci USA. 1978; 75: 4853–4857. [Medline] [CrossRef]
14. Schwarze U, Starman BJ, Byers PH. Redefinition of exon 7 in the *COL1A1* gene of type I collagen by an intron 8 splice-donor-site mutation in a form of osteogenesis imperfecta: influence of intron splice order on outcome of splice-site mutation. Am J Hum Genet. 1999; 65: 336–344. [Medline] [CrossRef]
15. Fortin A, Belouchi A, Tam MF, Cardon L, Skamene E, Stevenson MM, et al. Genetic control of blood parasitaemia in mouse malaria maps to chromosome 8. Nat Genet. 1997; 17: 382–383. [Medline] [CrossRef]
16. Mori M, Gotoh S, Taketani S, Hiai H, Higuchi K. Hereditary cataract of the Nakano mouse: Involvement of a hypomorphic mutation in the coproporphyrinogen oxidase gene. Exp Eye Res. 2013; 112: 45–50. [Medline] [CrossRef]
17. Liu C, Miyahara H, Dai J, Cui X, Li Y, Kang X, et al. Involvement of increased endoplasmic reticulum stress in the development of cataracts in BALB.NCT-*Cpox*^{nct} mice. Exp Eye Res. 2022; 215: 108905. [Medline] [CrossRef]
18. Cazzola M, Malcovati L. Diagnosis and treatment of sideroblastic anemias: from defective heme synthesis to abnormal RNA splicing. Hematology (Am Soc Hematol Educ Program). 2015; 2015: 19–25. [Medline] [CrossRef]
19. Méndez M, Moreno-Carralero MI, Morado-Arias M, Fernández-Jiménez MC, de la Iglesia Iñigo S, Morán-Jiménez MJ. Sideroblastic anemia: functional study of two novel missense mutations in *ALAS2*. Mol Genet Genomic Med. 2016; 4: 273–282. [Medline] [CrossRef]
20. Schmitt C, Gouya L, Malonova E, Lamoril J, Camadro JM, Flamme M, et al. Mutations in human *CPO* gene predict clinical expression of either hepatic hereditary coproporphyria or erythropoietic harderoporphyria. Hum Mol Genet. 2005; 14: 3089–3098. [Medline] [CrossRef]
21. Verra F, Mangano VD, Modiano D. Genetics of susceptibility to *Plasmodium falciparum*: from classical malaria resistance genes towards genome-wide association studies. Parasite Immunol. 2009; 31: 234–253. [Medline] [CrossRef]
22. Lelliott PM, McMorran BJ, Foote SJ, Burgio G. The influence of host genetics on erythrocytes and malaria infection: is there therapeutic potential? Malar J. 2015; 14: 289. [Medline] [CrossRef]
23. Ebel ER, Uricchio LH, Petrov DA, Egan ES. Revisiting the malaria hypothesis: accounting for polygenicity and pleiotropy. Trends Parasitol. 2022; 38: 290–301. [Medline] [CrossRef]
24. Ebel ER, Kuypers FA, Lin C, Petrov DA, Egan ES. Common host variation drives malaria parasite fitness in healthy human red cells. eLife. 2021; 10: e69808. [Medline] [CrossRef]
25. Goheen MM, Wegmüller R, Bah A, Darboe B, Danso E, Affara M, et al. Anemia offers stronger protection than sickle cell trait against the erythrocytic stage of *falciparum* malaria and this protection is reversed by iron supplementation. EBioMedicine. 2016; 14: 123–130. [Medline] [CrossRef]
26. Greth A, Lampkin S, Mayura-Guru P, Rodda F, Drysdale K, Roberts-Thomson M, et al. A novel ENU-mutation in ankyrin-1 disrupts malaria parasite maturation in red blood cells of mice. PLoS One. 2012; 7: e38999. [Medline] [CrossRef]
27. Huang HM, Bauer DC, Lelliott PM, Greth A, McMorran BJ, Foote SJ, et al. A novel ENU-induced ankyrin-1 mutation impairs parasite invasion and increases erythrocyte clearance during malaria infection in mice. Sci Rep. 2016; 6: 37197. [Medline] [CrossRef]
28. Lelliott PM, Huang HM, Dixon MW, Namvar A, Blanch AJ, Rajagopal V, et al. Erythrocyte β spectrin can be genetically targeted to protect mice from malaria. Blood Adv. 2017; 1: 2624–2636. [Medline] [CrossRef]